treat CAD. Although, there have been numerous improvements in the quality of stents, 5–10% of patients with drug-eluting stents still develop restenosis [1, 2]. This problem has led to routine use of the invasive and costly angiography for the surveillance of stent patency. Thus, a less invasive imaging technique for follow-up of patients with coronary stents is highly desirable.

With advances in temporal resolution [3] and volume coverage [4], the diagnostic accuracy of 64-slice MDCT for the detection of significant coronary artery stenosis has been reported to be high, especially in terms of the negative predictive value [5]. However, a recent study performed by 64-slice CT in 64 patients with 102 stents demonstrated that only 58% of the stents were evaluable, with the sensitivity of 86% and specificity of 98% among the evaluable stents [6]. A meta analysis study revealed that precise quantification of in-stent restenosis using 64-slice CT was not accurate[7]. As a result, ACCF/SCCT/ACR/AHA/ASE/ASNC/SCAI/SCMR 2010 Appropriate Use Criteria for Cardiac Computed Tomography ranked the evaluation of CAD with prior coronary stent with stent diameter $\leq$3 mm as inappropriate, and the evaluation of CAD with prior coronary stent and with stent diameter 3 mm as uncertain [8]. Implying that these techniques, in general, are not the most suitable or reasonable approaches for stent evaluation.

The results of earlier studies have indicated that spatial resolution is a key factor in the imaging of coronary artery stents [9]. Actually, in-stent restenosois is best determined by digital subtraction angiography because of the superior spatial resolution. High-Definition CT (HDCT: Discovery CT750 HD, GE Healthcare, WI, USA) has been developed recently, which theoretically implies improved spatial resolution. The purpose of this study was to evaluate the spatial resolution and in-stent lumen measurement accuracy of HDCT compared to conventional 64-slice CT (MDCT) using coronary stent phantoms.

Method and materials

Evaluation of the spatial resolution by the use of a slit phantom

A high-resolution insert of CATPHAN (The Phantom Laboratory, NY, USA) was placed at the iso-center of the scan plane, and scanned in the ECG-gated cardiac acquisition mode by both HDCT and 64-slice MDCT. The scanning protocol was: 64-row $\times$ 0.625 mm detector collimation, 120 kVp, 330 mA, 0.16:1 helical pitch, 0.35 s gantry rotation speed, and the images were reconstructed by the Detail reconstruction kernel with a thickness of 0.625 mm and display field-of-view (DFOV) of 96 mm.

Stent phantom

We developed six types of stent phantoms, ranging from 2.5 to 3.0 mm in diameter using three different types of stents (Bx-Velocity: Cordis/Johnson and Johnson; NJ USA, Driver: Medtronic; MN USA, Multilink-Rx: Guidant; CA USA). A 50% stenotic segment made of acrylic resin was built at the center inside the stent. All of these stents were placed inside simulated coronary arteries made of acrylic resin (Fig. 1). The lumen was filled with iodinated contrast material (Omnipaque 300, Daiichi-sankyo, Tokyo, Japan) and diluted with purified water to achieve 400 HU.

Scanning protocols

The stent phantoms were scanned by both HDCT and 64-slice MDCT in the ECG-gated cardiac helical mode under the following scanning conditions: 120 kVp, 300 mAs, 0.625 mm 0.16 helical pitch, and 0.35 s gantry rotation speed. Six types of stent phantoms were placed in a 15 $\times$ 25 cm^2 water tank, and positioned

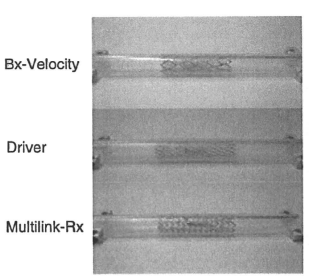

Fig. 1 Three different types of stents (Bx-Velocity, Driver, Multilink-Rx) which were placed inside simulated coronary arteries made of acrylic resin

along the Z-direction near the iso-center for both HDCT and the MDCT. CTDIvol at HDCT was 54.50 mGy and CTDIvol at MDCT was 56.16 mGy.

Data analysis

CT images were reconstructed under the following measurement conditions: 96 mm DFOV and Detail reconstruction kernel, 0.625 mm slice thickness with 0.3125 mm increments. Multiplanar reformatted longitudinal images with respect to the stent were obtained (Fig. 2). All the CT images were fixed at window width: 1,200, window level: 450. All data was transferred to a separate workstation. One observer (Y.T. with 7 years' experience in the interpretation of cardiac CT) measured the luminal diameter at the non-stenotic and stenotic segments of the stent phantom using digital calipers. We determined the mean luminal diameter (MLD) based on five measurements each obtained from different points. The underestimate ratio (UR) and △UR was defined as follows: UR = [True diameter of stent—MLD]/True diameter of stent; △UR = [MLD at HDCT—MLD at MDCT]/True diameter of stent.

Statistical analysis

All of the data were analyzed using SPSS version 15.0 (SPSS Inc., IL, USA) to compare the measurement values obtained using HDCT with those obtained using conventional 64-slice MDCT. *P*-values < 0.05 were considered to be statistically significant.

Results

Visual estimation of the slit phantom

The spatial resolution was estimated to be 0.71 mm for 64-slice MDCT and 0.50 mm for HDCT. The spatial resolution afforded by HDCT was approximately 30% ((0.71 − 0.50)/0.71) improved over that afforded by 64-slice MDCT in the cardiac mode (Fig. 3).

Stent phantom

The MLD of the 2.5- and 3.0-mm stents are shown in Tables 1 and 2. There was significant difference in the measured MLD between HDCT and 64-slice MDCT for all the stent phantoms (Fig. 4). At the non-stenotic segments, the △URs were 11.6% (Velocity), 16.4% (Driver) and 7.2% (Multilink) for the 2.5-mm stents, and 14.0% (Velocity), 16.3% (Driver) and 13.3% (Multilink) for the 3.0-mm stents. At the stenotic segment, the △URs were 23.2% (Velocity), 8.0% (Driver) and 13.6% (Multilink) for the 2.5-mm stents, and 20.0% (Velocity), 14.7% (Driver) and 15.3% (Multilink) for the 3.0-mm stents.

Discussion

Newly developed HDCT allowed high spatial resolution imaging. The keys of this high-resolution were improvements of Data Acquisition System (DAS),

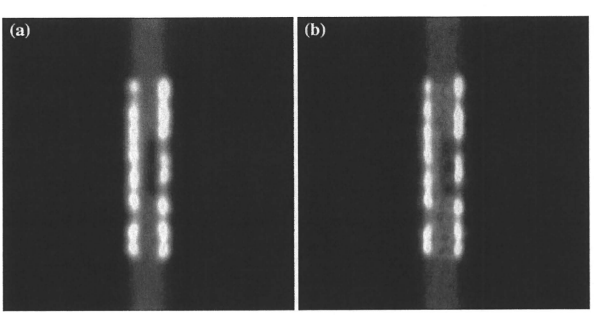

Fig. 2 Representative multiplanar reconstruction CT images of a stent (Velocity 3.0 mm) phantom are shown. **a** MDCT, **b** HDCT

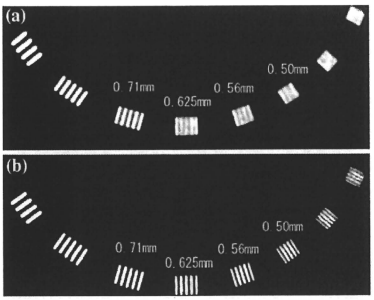

Fig. 3 Slit phantom on both scanners. **a** MDCT **b** HDCT. The spatial resolutions were estimated to be 0.71 mm for MDCT and 0.50 mm for HDCT

X-ray Tube and Detector. New DAS enabled 2496 sampling per rotation which was about 2.5 times of conventional sampling rate, which improved spatial resolution especially at the off-centered area. New X-ray tube equips dynamic deflecting of the focal spot which enabled double data sampling for azimuthal direction also improved spatial resolution in XY-plane imaging. The extremely rapid response of new detector (Gemstone^{TM}) enabled to take full advantage of the faster sampling of the DAS, and the dynamic focal spot deflection capability of the X-ray tube. The new detector had a primary decay time of only 30 microseconds, made it 100 times faster than the conventional scintillator material (GOS). Furthermore, levels of secondary decay of light emitting (afterglow) reached only 25% of GOS levels [10]. HDCT which had those three key technologies improved spatial resolution compared with conventional CT.

Visual estimation of the slit phantom in this study revealed an apparent spatial resolution of 0.50 mm on HDCT and 0.71 mm on 64-slice MDCT. Thus, the spatial resolution in HDCT was actually 30% improved as compared with that in conventional 64-slice MDCT. Min, et al., also reported that stent diameter without stenosis was higher with HDCT compared with MDCT, although, the stent with stenosis was not fully evaluated [11]. Our data using the stent phantom showed that the lumen visibility was 7.1–16.4% improved at the non-stenotic segment and 7.8–22.7% improved at the stenotic segment in HDCT compared with that in 64-slice MDCT. Sheth T, et al., reported that the assessment of restenosis of the coronary artery segments with stents was possible for only 33% of the 2.5-mm stents, while it was possible for a 100% of the 3.5- to 4.0-mm stents and 80% of the 3.0-mm stents [12]. Thus, MDCT was of limited usefulness for the assessment of 2.5-mm stents. Our data suggest that HDCT has the potential to improve the diagnostic performance of evaluation of in-stent restenosis.

Our study had some limitations. Firstly, our phantoms were static and motionless. Also the phantoms were imaged in water. Thus, some of the artifacts inherent in a true cardiac CT will be absent. The diagnostic performance of HDCT for in-stent restenosis remains unknown and further studies are necessary. Secondly, we could use only three types of stents; results could vary when other types of stents are used.

In conclusion, the spatial resolution of HDCT was approximately 30% improved over that of 64-slice MDCT in the cardiac mode. The superior spatial

Table 1 Mean luminal diameter (MLD) of 2.5-mm stents in MDCT and HDCT (mm)

	Velocity		Driver		Multilink	
	Non stenotic segment	Stenotic segment	Non stenotic segment	Stenotic segment	Non stenotic segment	Stenotic segment
MDCT	0.85 ± 0.06	0.30 ± 0.04	0.82 ± 0.06	0.48 ± 0.05	1.05 ± 0.03	0.37 ± 0.06
(UR*)	(66.0%)	(76.0%)	(67.2%)	(61.6%)	(58.0%)	(70.4%)
HDCT	1.14 ± 0.03	0.59 ± 0.06	1.23 ± 0.04	0.58 ± 0.02	1.23 ± 0.02	0.54 ± 0.01
(UR*)	(54.4%)	(52.8%)	(50.8%)	(53.6%)	(50.8%)	(56.8%)
△UR**	11.6%	23.2%	16.4%	8.0%	7.2%	13.6%

* UR:Underestimate ratio = [True diameter of stent—MLD]/True diameter of stent

** △UR = [MLD at HDCT—MLD at MDCT]/True diameter of stent

Table 2 Mean luminal diameter (MLD) of 3.0-mm stents in MDCT and HDCT(mm)

	Velocity		Driver		Multilink	
	Non stenotic segment	Stenotic segment	Non stenotic segment	Stenotic segment	Non stenotic segment	Stenotic segment
MDCT	1.57 ± 0.04	0.66 ± 0.06	1.42 ± 0.05	0.64 ± 0.05	1.48 ± 0.07	0.73 ± 0.05
(UR*)	(47.7%)	(56.0%)	(52.7%)	(57.3%)	(50.7%)	(51.3%)
HDCT	1.99 ± 0.12	0.96 ± 0.03	1.91 ± 0.04	0.86 ± 0.03	1.88 ± 0.04	0.96 ± 0.03
(UR*)	(33.7%)	(36.0%)	(36.3%)	(42.7%)	(37.3%)	(36.0%)
△UR**	14.0%	20.0%	16.3%	14.7%	13.3%	15.3%

* UR:Underestimate ratio = [True diameter of stent—MLD]/True diameter of stent

** △UR = [MLD at HDCT—MLD at MDCT]/True diameter of stent

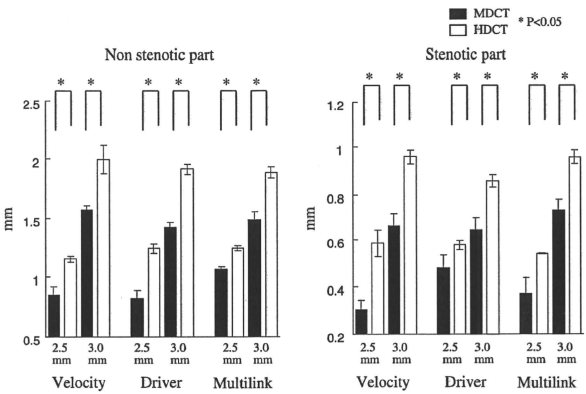

Fig. 4 The measurement values using HDCT were more accurate and significantly different from those obtained using conventional MDCT under every condition

resolution of HDCT could be promising for more accurate visualization inside a stent.

References

1. Morice MC, Colombo A, Meier B et al (2006) Sirolimus-vs paclitaxel-eluting stents in de novo coronary artery lesions: the REALITY trial: a randomized controlled trial. Jama 295:895–904
2. Holmes DR Jr., Leon MB, Moses JW et al (2004) Analysis of 1-year clinical outcomes in the SIRIUS trial: a randomized trial of a sirolimus-eluting stent versus a standard stent in patients at high risk for coronary restenosis. Circulation 109:634–640
3. Flohr TG, McCollough CH, Bruder H et al (2006) First performance evaluation of a dual-source CT (DSCT) system. Eur Radiol 16:256–268
4. Rybicki FJ, Otero HJ, Steigner ML et al (2008) Initial evaluation of coronary images from 320-detector row computed tomography. Int J Cardiovasc Imaging 24:535–546
5. Schroeder S, Achenbach S, Bengel F et al (2008) Cardiac computed tomography: indications, applications, limitations, and training requirements: report of a Writing Group deployed by the Working Group Nuclear Cardiology and Cardiac CT of the European Society of Cardiology and the European Council of Nuclear Cardiology. Eur Heart J 29:531–556
6. Rixe J, Achenbach S, Ropers D et al (2006) Assessment of coronary artery stent restenosis by 64-slice multi-detector computed tomography. Eur Heart J 27:2567–2572

7. Kumbhani DJ, Ingelmo CP, Schoenhagen P et al (2009) Meta-analysis of diagnostic efficacy of 64-slice computed tomography in the evaluation of coronary in-stent restenosis. Am J Cardiol 103:1675–1681
8. Taylor AJ, Cerqueira M, Hodgson JM et al (2010) ACCF/SCCT/ACR/AHA/ASE/ASNC/SCAI/SCMR 2010 Appropriate Use Criteria for Cardiac Computed Tomography. A Report of the American College of Cardiology Foundation Appropriate Use Criteria Task Force, the Society of Cardiovascular Computed Tomography, the American College of Radiology, the American Heart Association, the American Society of Echocardiography, the American Society of Nuclear Cardiology, the Society for Cardiovascular Angiography and Interventions, and the Society for Cardiovascular Magnetic Resonance. CARDIAC COMPUTED TOMOGRAPHY WRITING GROUP, Journal of the American College of Cardiology. J Am Coll Cardiol 56:1864–1894
9. Mahnken AH, Seyfarth T, Flohr T et al (2005) Flat-panel detector computed tomography for the assessment of coronary artery stents: phantom study in comparison with 16-slice spiral computed tomography. Invest Radiol 40:8–13
10. Vartuli JS, Lyons RJ, Vess CJ et al (2008) GE Healthcare's New Computed Tomography Scintillator—Gemstone. Symposium on Radiation Measurement and Applications, June 2–5, Berkeley, California
11. Min JK, Swaminathan RV, Vass M et al (2009) High-definition multidetector computed tomography for evaluation of coronary artery stents: comparison to standard-definition 64-detector row computed tomography. J Cardiovasc Comput Tomogr 3:246–251
12. Sheth T, Dodd JD, Hoffmann U et al (2007) Coronary stent assessability by 64 slice multi-detector computed tomography. Catheter Cardiovasc Interv 69:933–938

International Journal of Cardiology xxx (2011) xxx–xxx

Contents lists available at ScienceDirect

International Journal of Cardiology

journal homepage: www.elsevier.com/locate/ijcard

Association between epicardial adipose tissue volume and characteristics of non-calcified plaques assessed by coronary computed tomographic angiography

Toshiharu Oka [a], Hideya Yamamoto [a,*], Norihiko Ohashi [a], Toshiro Kitagawa [a], Eiji Kunita [a], Hiroto Utsunomiya [a], Ryo Yamazato [a], Yoji Urabe [a], Jun Horiguchi [b], Kazuo Awai [c], Yasuki Kihara [a]

[a] Department of Cardiovascular Medicine, Hiroshima University, Graduate School of Biomedical Sciences, Hiroshima, Japan
[b] Department of Clinical Radiology, Hiroshima University Hospital, Hiroshima, Japan
[c] Department of Diagnostic Radiology, Hiroshima University, Graduate School of Biomedical Sciences, Hiroshima, Japan

ARTICLE INFO

Article history:
Received 11 December 2010
Received in revised form 1 April 2011
Accepted 24 April 2011
Available online xxxx

Keywords:
Cardiac computed tomography
Epicardial adipose tissue
Low-density plaque
Positive remodeling

ABSTRACT

Background: The aim of this study was to investigate whether high epicardial adipose tissue (EAT) volume is related to the presence of vulnerable coronary plaque components as assessed by computed tomography (CT).

Methods: We evaluated 357 patients referred for 64-slice CT, and assessed coronary plaque components and EAT volume. Vulnerable coronary plaque components were defined as the presence of non-calcified plaque (NCP), including low-density plaque (LDP: <39 HU) and positive remodeling (PR: remodeling index >1.05). In accordance with a previous report, patients were assigned to two groups: low (<100 ml) or high (≥100 ml) EAT volume.

Results: Compared to the low EAT volume group, the high EAT volume group had a higher prevalence of NCP (74% vs. 59%, $p=0.003$). Additionally, the high EAT volume group had a higher prevalence of LDP with PR than the low EAT volume group (46% vs. 25%, $p<0.001$). Interestingly, a high EAT volume was an independent predictor of LDP with PR (odds ratio 2.56, 95% confidence interval 1.38–4.85, $p=0.003$) after adjusting for age, gender, traditional cardiovascular risk factors, body mass index (BMI), abdominal visceral adipose tissue (VAT), and coronary artery calcium (CAC) scores.

Conclusions: A high EAT volume was associated with the presence of vulnerable plaque components, independent of obesity measurements (BMI and VAT) and CAC scores.

1. Introduction

Several studies have demonstrated that excessive fat accumulation in abdominal viscera is associated with coronary artery disease (CAD), myocardial infarction, and cardiovascular mortality [1, 2]. In our previous studies using computed tomography (CT), abdominal visceral adipose tissue (VAT) was a critical and independent determinant for, not only the presence, but also the extent of coronary artery calcium (CAC) scores [3]. This was also a determinant for non-calcified coronary plaques (NCPs) [4]. It has been reported that both epicardial and abdominal adipocytes are derived from the splanchnopleuric mesoderm, and that adipokines derived from the epicardial adipose tissue (EAT) surrounding coronary arteries may directly affect vessel walls, as well as the progress of atherosclerosis [5].

Recent advances in cardiac CT technology have enabled the identification and characterization of NCPs. Plaque components and vascular remodeling can be reliably assessed by 64-slice CT angiography, and NCPs with low CT density and positive remodeling (PR) frequently co-exist in potentially vulnerable lesions [6-8]. Although several studies have suggested that EAT is associated with CAC scores and coronary artery disease [9, 10], the association between EAT and NCPs remains unclear. The aim of the present study was to investigate the relationships between EAT volume and the presence of NCP vulnerable components, as defined by CT angiography.

2. Methods

2.1. Subjects

Between December 2007 and April 2009, a total of 495 consecutive patients with suspected CAD underwent a 64-slice CT assessment at our institution. For the present study, we excluded 138 subjects with a history of coronary revascularization ($n=110$), inadequate image quality because of motion artifacts or inadequate contrast concentration ($n=18$), or with missing information for one or more traditional CAD risk factors ($n=10$). Eventually, 357 patients were included in this study. In all patients, plain cardiac and abdominal scans were performed to measure the CAC scores

* Corresponding author at: Department of Cardiovascular Medicine, Hiroshima University, Graduate School of Biomedical Sciences, 1-2-3 Kasumi Minami-ku, Hiroshima 734-8551, Japan. Tel.: +81 82 257 5540; fax: +81 82 257 1569.
E-mail address: hideyayama@hiroshima-u.ac.jp (H. Yamamoto).

0167-5273/$ – see front matter © 2011 Elsevier Ireland Ltd. All rights reserved.
doi:10.1016/j.ijcard.2011.04.021

Please cite this article as: Oka T, et al, Association between epicardial adipose tissue volume and characteristics of non-calcified plaques assessed by coronary computed tomographic angiography, Int J Cardiol (2011), doi:10.1016/j.ijcard.2011.04.021

and the VAT areas. The study protocol was approved by the Ethical Committee at Hiroshima University, and written informed consent was obtained from all patients.

2.2. Risk factor assessments

All patients provided detailed clinical information at their clinical consultation. Hypertension was defined as a patient systolic blood pressure ≥ 140 mmHg, a diastolic blood pressure ≥ 90 mmHg, or the current use of antihypertensive medications. Hypercholesterolemia was defined as a low-density lipoprotein (LDL) cholesterol level ≥ 140 mg/dl on direct measurement, a total cholesterol level ≥ 220 mg/dl, or the current use of lipid-lowering drugs. Diabetes mellitus (DM) was defined by self-reporting, a glycohemoglobin A1c (HbA1c) level ≥ 6.5% [11], or the current use of hypoglycemic agents. Patients who smoked regularly during the previous year were classified as current smokers.

2.3. CT angiography and image analysis

CT examinations were performed using a 64-slice CT scanner (LightSpeed VCT, GE Healthcare, Waukesha, Wisconsin, USA). Patients orally received 40 mg metoprolol 60 min before CT scanning if the patient's resting heart rate was >60 beats/min; all patients received 0.3 mg nitroglycerin just before scanning. Prior to CTA, 35–40 contiguous images were obtained with a 2.5-mm slice thickness to measure the CAC scores, according to the Agatston method [12]. Contrast-enhanced scanning, and the scan protocol and reconstruction methods, were performed, as previously described [6, 7]. The effective radiation dose was estimated based on the dose-length product, and ranged from 15 to 18 mSv. Image reconstruction was performed using the CardIQ image analysis software program (GE Healthcare) on a dedicated computer workstation (Advantage Workstation Ver.4.2, GE Healthcare).

2.4. Plaque characterization

All coronary segments >2 mm in diameter were evaluated by two experienced independent observers using curved multi-planar reconstructions and cross-sectional images rendered perpendicularly to the vessel center line. CAD was defined by a cross-sectional narrowing >50% in epicardial coronary arteries.

Atherosclerotic plaques were classified as calcified or non-calcified. Calcified plaques were defined as lesions composed exclusively of structures with a CT density greater than that of the contrast-enhanced coronary lumen, or with a CT density >130 HU assigned to the coronary artery wall in a plain image. NCPs were defined as a low-density mass >1 mm^2 in size located within the vessel wall and clearly distinguishable from the contrast-enhanced coronary lumen and the surrounding pericardial tissue. In regard to the extent of calcified plaque and NCP, a high plaque count was defined as ≥ 2, and a low plaque count as ≤ 1. We further evaluated the NCP components by determining the minimal CT density, the vascular remodeling index (RI), and adjacent coronary calcium, as previously described [6, 7]. Briefly, the minimum CT density was determined to be the lowest average value of at least five regions of interest (area = 1 mm^2). A low-density plaque (LDP) was defined as a lesion with a minimum CT density <39 HU [6, 7]. Vascular remodeling was assessed using the RI, which was calculated by dividing the cross-sectional lesion vessel area by the proximal reference vessel area. Positive remodeling (PR) was defined as a RI > 1.05 [6, 7]. Spotty calcium was defined as calcium burden length < 3/2 of the vessel diameter and a width < 2/3 of the vessel diameter.

2.5. Measurement of VAT area and EAT volume using CT

Abdominal scans were performed at the 4th and 5th lumbar levels in the spinal position. The VAT area was defined as the intraperitoneal adipose tissue area at the level of umbilicus using commercial software (Virtual Place, AZE INC., Tokyo, Japan) [3, 4].

Using cross-sectional CT images for calcium scoring, EAT was defined as the adipose tissue between the epicardial surface of the myocardium and the pericardium. The EAT area within the manually traced epicardium was defined as having a density range between −250 and −30 HU and was automatically quantified using the same software as for the VAT area. EAT volume was calculated as the total sum of the EAT areas from the atrial appendage (i.e. 1 cm above the left main coronary artery) to the apex with 1 cm thick spacing between each image, as was previously described [10]. Based on the findings of Sarin et al. [10], a cut-off value of 100 ml for EAT volume was used, and patients were assigned to two groups, either the low (<100 ml) or the high (≥ 100 ml) EAT volume group. Intra- and inter-observer variability for the quantification of EAT volumes were calculated by the formula as previously reported [13].

2.6. Statistical analysis

Categorical variables are presented as the numbers of patients (percentage), and continuous variables are expressed as means ± SD or medians (interquartile range). For each variable, differences were evaluated using the Pearson χ^2-tests for categorical variables and the Student *t* test or the Mann–Whitney *U* test for continuous variables. We then assessed whether the associations between high EAT volume and the presence of NCP components were independent of age, gender, traditional coronary risk factors, BMI, VAT area, and CAC scores via multivariate logistic regression analyses. All analyses were performed using the JMP 8.0.2 software program (SAS Institute, Tokyo, Japan). *P* values < 0.05 were considered to be statistically significant.

3. Results

3.1. Patient characteristics and EAT volume measurement

The mean age of the study population was 66 ± 11 years old, and 64% of the subjects were male. The prevalence of coronary risk factors was as follows: hypertension (68%), hypercholesterolemia (50%), DM (31%), and smoking (31%). The mean BMI was 24.2 ± 4.8 kg/m^2. A total of 124 patients (35%) had CAD. The mean EAT volume was 125 ± 44 ml.

Baseline clinical characteristics and CT quantification are listed in Table 1. The high EAT volume group had higher BMIs, VAT areas, percentage of patients who were current smokers, and proportion of individuals with DM compared to the low EAT volume group. The prevalence of patients with CAD and a CAC score >0 was higher in the high EAT volume group than in the low EAT volume group (38% vs. 26%, $p = 0.026$, 78% vs. 64%, $p = 0.005$, respectively). In comparison to the low EAT volume group, the high EAT volume group had a higher prevalence and extent (≥ 2 counts) of calcified plaques (70% vs. 58%, $p = 0.027$, and 54% vs. 41%, $p = 0.026$, respectively) and NCPs (74% vs. 59%, $p = 0.003$, and 52% vs. 40%, $p = 0.041$, respectively). Fig. 1 shows the comparison of NCP with vulnerable plaque components in patients with low vs. high EAT volume. The high EAT volume group had a higher prevalence of LDP (52% vs. 27%, $p < 0.001$), PR (58% vs. 37%, $p < 0.001$), and LDP with PR (46% vs. 25%, $p < 0.001$) compared to the low EAT volume group. Intra- and inter-observer variability for the quantification of EAT volumes were 3.0% and 4.8%, respectively.

3.2. Relationship between high EAT volume and the presence of NCP vulnerable components

Table 2 shows the results of age and sex-adjusted and multivariate analyses of the relationships between high EAT volume and NCP components. After adjusting for age, gender, hypertension, DM, smoking, BMI, and VAT area, Model-1 shows that high EAT volume

Table 1
Baseline characteristics and CT findings in patients with low and high EAT volume ($n = 357$).

Characteristics	Low EAT volume (<100 ml)	High EAT volume (≥ 100 ml)	*p* value
	$n = 107$	$n = 250$	
Age (years)	64.2 ± 11.1	66.3 ± 10.7	0.090
Male gender	63 (59)	165 (66)	0.199
Body mass index (kg/m^2)	22.0 ± 2.9	25.1 ± 5.2	<0.001
Hypercholesterolemia	50 (47)	128 (51)	0.44
Family history	17 (17)	37 (16)	0.79
Current smoker	24 (22)	86 (34)	0.025
Hypertension	66 (62)	176 (70)	0.11
Diabetes mellitus	21 (20)	90 (36)	0.002
Total cholesterol (mg/dl)	199.1 ± 38.1	201.3 ± 35.9	0.60
Triglyceride (mg/dl)	137.5 ± 100.8	154.7 ± 86.1	0.10
LDL cholesterol (mg/dl)	115.3 ± 32.4	120.7 ± 29.7	0.13
HDL cholesterol (mg/dl)	62.6 ± 18.1	58.0 ± 17.9	0.026
HbA1c (%)	5.71 ± 1.24	5.98 ± 1.01	0.029
VAT area (cm^2)	74.9 ± 35.1	120.6 ± 45.6	<0.001
Coronary artery disease	28 (26)	96 (38)	0.026
CAC scores	46 (0–236)	54 (0–242)	0.50
CAC scores >0	68 (64)	194 (78)	0.005
Calcified plaque	62 (58)	175 (70)	0.027
Calcified plaque counts ≥ 2	44 (41)	135 (54)	0.026
Non-calcified plaque	63 (59)	186 (74)	0.003
Non-calcified plaque counts ≥ 2	43 (40)	130 (52)	0.041

Values are expressed as number (percent), mean ± SD, or median (interquartile range). LDL: low-density lipoprotein; HDL: high-density lipoprotein; HbA1c: glycohemoglobin A1c; VAT: visceral adipose tissue; CAC: coronary artery calcium.

Please cite this article as: Oka T, et al, Association between epicardial adipose tissue volume and characteristics of non-calcified plaques assessed by coronary computed tomographic angiography, Int J Cardiol (2011), doi:10.1016/j.ijcard.2011.04.021

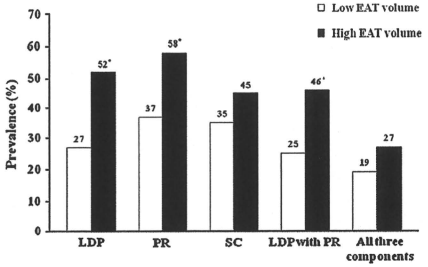

Fig. 1. Comparison of vulnerable plaque components in patients with low vs. high EAT volume.LDP: low-density plaque; PR: positive remodeling; SC: spotty calcium.* $p<0.05$ vs. low EAT volume group.

was independently associated with the presence of LDP (OR 2.90, 95% CI 1.59–5.42, $p<0.001$), PR (OR 1.94, 95% CI 1.07–3.54, $p=0.030$), and LDP with PR (OR 2.42, 95% CI 1.32–4.51, $p=0.005$). After adjusting for the variables in Model-1, as well as CAC scores, Model-2 shows that high EAT volume was still an independent predictor for the presence of LDP (OR 3.08, 95% CI 1.66–5.83, $p<0.001$), PR (OR 2.08, 95% CI 1.12–3.88, $p=0.021$), and LDP with PR (OR 2.56, 95% CI 1.38–4.85, $p=0.003$). Fig. 2 shows a representative case with high EAT volume presenting vulnerable plaque components.

4. Discussion

The present study demonstrates the relationships between coronary NCP components and EAT volume as measured by CT. The data indicate that a high accumulation of EAT is associated with the existence of NCP components (considered to be rupture-prone vulnerable features of plaque) after adjustment for other obesity measurements (BMI and VAT area) and CAC scores. The EAT measurement may provide novel and additional risk stratification for patients suspected of coronary artery disease.

4.1. EAT measurement

In the present study, we have demonstrated that EAT volume by CT is noninvasively measured and had a high reproducibility. Recently, several studies have shown that cardiac CT scans and magnetic resonance imaging can quantify EAT volume with high reproducibility, and are thereby effective tools for measuring EAT volume [10, 13-16]. In our CT study, using plane axial slices for calcium scoring, patients could obtain additional clinical information of risk stratification without additional radiation exposure or cost.

Our methods of measuring EAT volume can be utilized to evaluate the amount of adipose tissue surrounding coronary arteries. Using an EAT volume cut-off of 100 ml, which was based on the findings of Sarin et al. [10], we were able to detect LDP with PR at a sensitivity of 80%, a specificity of 41%, and an accuracy of 57%. Thus, the EAT volume cut-off of 100 ml is highly sensitivity, and can be used as a screening tool for detecting NCP with vulnerable coronary plaque components.

On the other hand, an echocardiographic study has shown the relationship between EAT thickness and coronary atherosclerosis [17]. Saura et al. [18] showed that EAT thickness measured by echocardiography had a poor reproducibility. Although transthoracic echocardiography is a simple and easy method to assess EAT volume, it is difficult to distinguish between small amounts of EAT and pericardial effusion and to measure EAT accurately in obese patients due to their poor echo images.

4.2. The relationship between EAT and coronary atherosclerosis

We revealed that high EAT volume was associated with not only the presence of CAD but also that of vulnerable plaque components. Several previous studies have demonstrated that high EAT volume was related to the existence of CAD [10] or myocardial ischemia as assessed by single photon emission computed tomography [19]. According to these findings, the accumulation of EAT around coronary arteries may contribute to the development of coronary atherosclerosis.

Several studies have reported the relationships between EAT volume and coronary plaque components. Konishi et al. [13] showed that high EAT volume was independently and significantly associated with the presence of coronary plaques, especially non-stenotic and non-calcified plaques using 64-slice CT. Alexopoulos et al. [20] have demonstrated that EAT volume was greater in patients with mixed and non-calcified plaques than in patients without plaques. In the present study, we assessed more detailed plaque components of coronary plaques than previous studies. Interestingly, we clarified that a high EAT volume was associated with the presence of LDP with PR. We found clinical significance when evaluating the EAT volume to predict patients at a high risk for vulnerable plaque components, which may contribute to acute coronary syndrome [6-8]. In a sub-analysis of the Multi-Ethnic Study of Atherosclerosis, a high pericardial adipose tissue volume was also associated with future incident coronary heart disease [21], which is consistent with our results.

Notably, our results revealed that higher EAT volumes are associated with the presence of LDP with PR after adjusting for BMI and VAT area. It was reported that the EAT thickness was associated with an increasing number of CAD lesions after adjusting for conventional risk factors, BMI, and VAT [16]. Consistent with our results, several reports have shown that EAT accumulation is associated with CAD and CAC scores in non-obese patients [22, 23]. Further, our results suggest that a high EAT volume is an independent predictor for vulnerable plaque components even after adjusting for CAC scores. Thus, EAT volume measurements, along with CAC scores, could be used to predict whether a patient is at high risk for vulnerable plaque components. The local effect of EAT on coronary arteries may play an important role in plaque formation. It can be speculated that a high EAT volume may be a direct and intimate

Table 2
Relationship between high epicardial adipose tissue volume and non-calcified plaque components.

Plaque components	Age and sex-adjusted		Multivariate (Model-1)[a]		Multivariate (Model-2)[b]	
	OR (95% CI)	*p* value	OR (95% CI)	*p* value	OR (95% CI)	*p* value
Low-density plaque	2.66 (1.60–4.49)	<0.001	2.90 (1.59–5.42)	<0.001	3.08 (1.66–5.83)	<0.001
Positive remodeling	2.08 (1.28–3.42)	0.004	1.94 (1.07–3.54)	0.030	2.08 (1.12–3.88)	0.021
Spotty calcium	1.34 (0.82–2.23)	0.25	1.08 (0.59–1.97)	0.80	1.11 (0.61–2.04)	0.73
Low-density plaque with positive remodeling	2.36 (1.42–4.02)	0.001	2.42 (1.32–4.51)	0.005	2.56 (1.38–4.85)	0.003
All three characteristics	1.42 (0.80–2.58)	0.24	1.49 (0.75–3.02)	0.26	1.65 (0.81–3.44)	0.17

OR: odds ratio; CI: confidence interval.
[a] Adjusted for age, sex, hypertension, hypercholesterolemia, diabetes mellitus, current smoking, body mass index, and visceral adipose tissue area.
[b] Adjusted for variables in Model-1 and CAC scores.

Please cite this article as: Oka T, et al, Association between epicardial adipose tissue volume and characteristics of non-calcified plaques assessed by coronary computed tomographic angiography, Int J Cardiol (2011), doi:10.1016/j.ijcard.2011.04.021

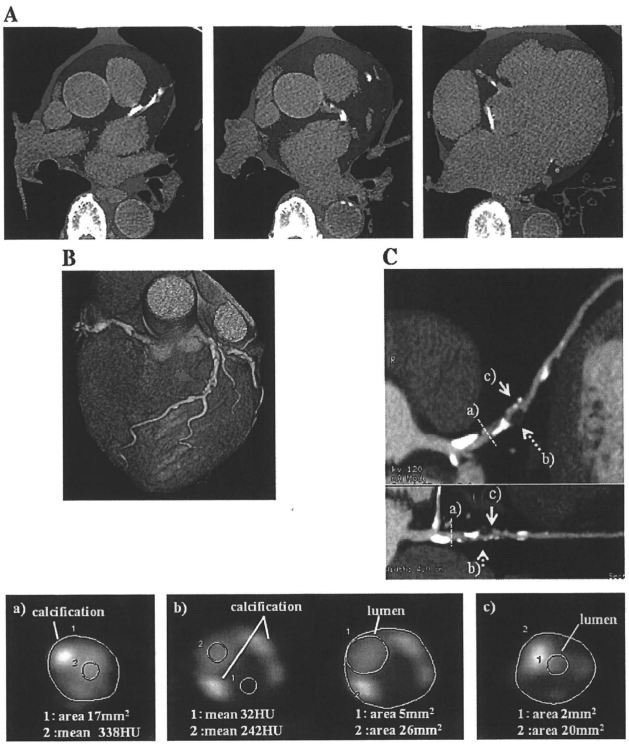

Fig. 2. A representative case with high accumulation of EAT presenting coronary atherosclerotic plaque with vulnerable plaque components.A density range between −250 and −30 HU was assigned as the adipose tissue. The EAT area (blue area) was manually traced on the epicardium (panel A). In this case, the EAT volume was 216 ml. The volume rendering image shows an atherosclerotic lesion in the middle portion of the left anterior descending artery (LAD) (panel B, blue arrow). The multi-planar reconstruction image of LAD shows an obstructive non-calcified plaque lesion with low-density plaque, positive vascular remodeling, and adjacent spotty calcium (panel C). The remodeling index is 1.53, calculated from the cross-sectional images of the reference site (a) and the lesion site (b). The minimum CT density of the lesion site is 32 HU. Adjacent spotty calcium can be observed in the cross-sectional image (a,b, and c).

source of adipokines, and thereby abnormal adipokine signaling in and around the coronary arteries. As in our previous report [4], high VAT area is significantly associated with NCP vulnerable components. We believe that VAT and EAT may work synergistically to accelerate coronary atherosclerosis and plaque vulnerability from inside and from outside the vessel walls, respectively.

4.3. Limitations

In the present study, we could not measure serum or tissue inflammatory cytokines and adipokines, both of which can lead to accelerate atherosclerosis or plaque vulnerability. A previous study demonstrated that the EAT in patients with critical CAD had a higher expression level of inflammatory mediators compared with subcutaneous adipose tissues, but the circulating inflammatory biomarkers were not correlated with overall biomarker expression [24]. Therefore, further studies will be necessary to clarify the relationship between the tissue inflammatory cytokine or adipokine levels and EAT volume.

Finally, the present study may have been affected by selection bias, because the study was composed of patients with suspected CAD. In addition, this was a cross-sectional study with a relatively small sample size.

5. Conclusions

EAT accumulation was associated with the presence of coronary plaques with vulnerable characteristics, as detected by coronary CT angiography. A high EAT volume is a predictor of vulnerable plaque components independent of obesity measurements (BMI and VAT) and CAC scores.

Acknowledgments

The authors of this manuscript have certified that they comply with the Principles of Ethical Publishing in the International Journal of Cardiology [25].

Please cite this article as: Oka T, et al, Association between epicardial adipose tissue volume and characteristics of non-calcified plaques assessed by coronary computed tomographic angiography, Int J Cardiol (2011), doi:10.1016/j.ijcard.2011.04.021

This study was supported by the Tsuchiya Foundation, Hiroshima, Japan.

References

[1] See R, Abdullah SM, McGuire DK, et al. The association of differing measures of overweight and obesity with prevalent atherosclerosis: the Dallas Heart Study. J Am Coll Cardiol 2007;50:752–9.
[2] Yusuf S, Hawken S, Ounpuu S, et al. Obesity and the risk of myocardial infarction in 27,000 participants from 52 countries: a case-control study. Lancet 2005;366: 1640–9.
[3] Ohashi N, Yamamoto H, Horiguchi J, et al. Visceral fat accumulation as a predictor of coronary artery calcium as assessed by multislice computed tomography in Japanese patients. Atherosclerosis 2009;202:192–9.
[4] Ohashi N, Yamamoto H, Horiguchi J, et al. Association between visceral adipose tissue area and coronary plaque morphology assessed by CT angiography. JACC Cardiovasc Imaging 2010;3:908–17.
[5] Sacks HS, Fain JN. Human epicardial adipose tissue: a review. Am Heart J 2007;153:907–17.
[6] Kitagawa T, Yamamoto H, Ohhashi N, et al. Comprehensive evaluation of noncalcified coronary plaque characteristics detected using 64-slice computed tomography in patients with proven or suspected coronary artery disease. Am Heart J 2007;154:1191–8.
[7] Kitagawa T, Yamamoto H, Horiguchi J, et al. Characterization of noncalcified coronary plaques and identification of culprit lesions in patients with acute coronary syndrome by 64-slice computed tomography. JACC Cardiovasc Imaging 2009;2:153–60.
[8] Motoyama S, Sarai M, Harigaya H, et al. Computed tomographic angiography characteristics of atherosclerotic plaques subsequently resulting in acute coronary syndrome. J Am Coll Cardiol 2009;54:49–57.
[9] Djaberi R, Schuijf JD, van Werkhoven JM, Nucifora G, Jukema JW, Bax JJ. Relation of epicardial adipose tissue to coronary atherosclerosis. Am J Cardiol 2008;102: 1602–7.
[10] Sarin S, Wenger C, Marwaha A, et al. Clinical significance of epicardial fat measured using cardiac multislice computed tomography. Am J Cardiol 2008;102: 767–71.
[11] International Expert Committee. International Expert Committee report on the role of the A1C assay in the diagnosis of diabetes. Diabetes Care 2009;32:1327–34.
[12] Agatston AS, Janowitz WR, Hildner FJ, Zusmer NR, Viamonte Jr M, Detrano R. Quantification of coronary artery calcium using ultrafast computed tomography. J Am Coll Cardiol 1990;15:827–32.
[13] Konishi M, Sugiyama S, Sugamura K, et al. Association of pericardial fat accumulation rather than abdominal obesity with coronary atherosclerotic plaque formation in patients with suspected coronary artery disease. Atherosclerosis 2010;209:573–8.
[14] Nelson AJ, Worthley MI, Psaltis PJ, et al. Validation of cardiovascular magnetic resonance assessment of pericardial adipose tissue volume. J Cardiovasc Magn Reson 2009;11:15.
[15] Perseghin G, Lattuada G, De Cobelli F, et al. Increased mediastinal fat and impaired left ventricular energy metabolism in young men with newly found fatty liver. Hepatology 2008;47:51–8.
[16] Wang TD, Lee WJ, Shih FY, et al. Association of epicardial adipose tissue with coronary atherosclerosis is region-specific and independent of conventional risk factors and intra-abdominal adiposity. Atherosclerosis 2010;213:279–87.
[17] Iacobellis G, Lonn E, Lamy A, Singh N, Sharma AM. Epicardial fat thickness and coronary artery disease correlate independently of obesity. Int J Cardiol in press.
[18] Saura D, Oliva MJ, Rodriguez D, et al. Reproducibility of echocardiographic measurements of epicardial fat thickness. Int J Cardiol 2010;141:311–3.
[19] Tamarappoo B, Dey D, Shmilovich H, et al. Increased pericardial fat volume measured from noncontrast CT predicts myocardial ischemia by SPECT. JACC Cardiovasc Imaging 2010;3:1104–12.
[20] Alexopoulos N, McLean DS, Janik M, Arepalli CD, Stillman AE, Raggi P. Epicardial adipose tissue and coronary artery plaque characteristics. Atherosclerosis 2009;213:150–4.
[21] Ding J, Hsu FC, Harris TB, et al. The association of pericardial fat with incident coronary heart disease: the Multi-Ethnic Study of Atherosclerosis (MESA). Am J Clin Nutr 2009;90:499–504.
[22] Yong HS, Kim EJ, Seo HS, et al. Pericardial fat is more abundant in patients with coronary atherosclerosis and even in the non-obese patients: evaluation with cardiac CT angiography. Int J Cardiovasc Imaging 2009;26:53–62.
[23] Gorter PM, de Vos AM, van der Graaf Y, et al. Relation of epicardial and pericoronary fat to coronary atherosclerosis and coronary artery calcium in patients undergoing coronary angiography. Am J Cardiol 2008;102:380–5.
[24] Mazurek T, Zhang L, Zalewski A, et al. Human epicardial adipose tissue is a source of inflammatory mediators. Circulation 2003;108:2460–6.
[25] Shewan LG, Coats AJ. Ethics in the authorship and publishing of scientific articles Int J Cardiol 2010;144:1–2.

Please cite this article as: Oka T, et al. Association between epicardial adipose tissue volume and characteristics of non-calcified plaques assessed by coronary computed tomographic angiography. Int J Cardiol (2011), doi:10.1016/j.ijcard.2011.04.021